



## A QSAR Study of 2-carboxamide-1,4-di-N-oxide quinoxaline Derivatives

Mohamad Reza Talei Bavil Olyai<sup>1</sup>, Hadi Behzadi<sup>2</sup>, Payman Roonasi<sup>2</sup>, Khaton Taghipour<sup>2</sup>

<sup>1</sup>Department of Chemistry, Faculty of Science, Islamic Azad University, Karaj Branch, Karaj, Alborz, Iran

<sup>2</sup>Department of Chemistry, Kharazmi University, Karaj, Tehran, Iran

(Received 10 Mar. 2015; Final version received 15 Jun. 2015)

### Abstract

A set of density functional theory (DFT) calculations were performed on 2-carboxamide-1,4-di-N-oxide quinoxaline (2CdNOQ) derivatives. The optimized structure of these compounds in three forms was obtained. Some electronic parameters including dipole moment ( $\mu$ ), ionization potential ( $I$ ), electron affinity ( $A$ ), LUMO energy ( $\epsilon_{\text{LUMO}}$ ), HOMO energy ( $\epsilon_{\text{HOMO}}$ ), electronegativity ( $\chi$ ), hardness ( $\eta$ ), electrophilicity ( $\omega$ ), and differences between HOMO and LUMO energies ( $\epsilon_{\text{LUMO}} - \epsilon_{\text{HOMO}}$ ), for the most stable conformer, were calculated. Quantitative structure–activity relationship (QSAR) models of the biological activity (IC<sub>50</sub>) of these compounds were established using the calculated quantum mechanical descriptors. Also, the first, second, total, and mean N-O bond dissociation enthalpies were also obtained theoretically and were correlated to reported experimental inhibition.

**Key words:** QSAR study, Quinoxaline derivatives, Anti-tuberculous activity, DFT calculations, IC<sub>50</sub>.

### Introduction

Tuberculosis (TB) is a respiratory transmitted disease affecting nearly 32% of the world's population, more than any other infectious disease. TB is caused by Mycobacterium Tuberculosis (M.Tbc) and the statistics indicate that 1.6 million people throughout the world die

from Tuberculosis [1]. In addition, the statistics showed that an estimated 8.8 million new cases emerged in 2005; 34% of these cases occurred in the South-East Asia region [1]. One-third of the population is infected with M. Tuberculosis and the World Health Organization (WHO) estimates that within the next 20 years about

\* Corresponding author: Dr Mohamad Reza Talei Bavil Olyai, Department of Chemistry, Faculty of Science, Islamic Azad University, Karaj Branch, P. O. Box 31485-313, Karaj, Alborz, Iran. Email: talei3@azad.ac.ir; Phone No.: +982614182305, Fax: +982614418156.

30 million people will be infected with the bacillus [2]. The development of resistance by *M. tuberculosis* to commonly used anti-tuberculosis drugs, the increasing incidences of disease in immuno-compromised patients, and longer durations of therapy, highlights the need for new drugs to extend the range of effective TB treatment options [3]. One of five lead compound series which were identified and are currently being pursued under the Tuberculosis Antimicrobial Acquisition and Coordinating Facility (TAACF) program is the series of quinoxaline 1,4-di-N-oxide derivatives

[4]. Quinoxaline derivatives are a class of compounds that show very interesting biological properties and the interest in these compounds is growing within the field of medicinal chemistry. Specifically, 2-carboxamide-1,4-di-N-oxide-Quinoxaline derivatives (Figure 1) even improve the biological results shown by their reduced analogues and are endowed with antiviral, anticancer, antibacterial and antiprotozoal activities [5-9]. In addition, it is observed that the absence of the two N-oxide groups generally led to the loss of the antimycobacterial activity [8, 10].

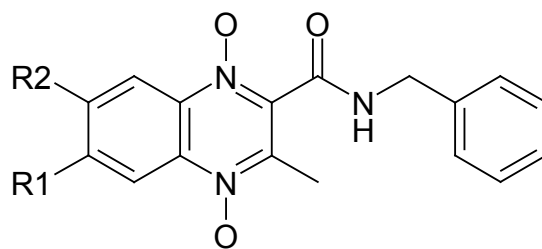


**Figure 1.** General structure of 2-carboxamide-1,4-di-N-oxide quinoxaline (2CdNOQ) derivatives.

Nowadays, an alternative way for overcoming the absence of experimental measurements for biological systems is based on the ability to formulate quantitative structure–activity relationships (QSARs) [11, 12]. QSAR is a mathematical representation of biological activity in terms of structural descriptors of a series of homologue molecules [13-18]. The main objective of QSAR is to look for new molecules with required properties using chemical intuition and experience transformed into a mathematically quantified and computerized form [18]. Thus QSAR methodology saves resources and expedites

the process of development of new molecules and drugs [19,20]. Success of QSAR in the development of new drug molecules and prediction of toxicity of molecules is highly appreciable [13-18]. Quantum chemical descriptors have extensively been used in QSAR studies in biochemistry.

This study was performed using density functional theory (DFT) method for modeling and estimating TB inhibition by 2-carboxamide-1, 4-di-N-oxide-Quinoxalinederivatives (2CdNOQ). The first is to build QSAR linear regression models using DFT-based descriptors and to correlate

and predict the inhibition constant (IC50) for a diverse set of 2-carboxamide-1, 4-di-N-oxide-Quinoxaline compounds. The IC50 values of compounds were taken from study [21]. This study has employed DFT method using B3LYP hybrid functional together with 6-31+G(d) basis set to calculate various quantum mechanical descriptors and correlated them using the reported experimental inhibition constants employing multi linear regression models. In addition, the N-O bond strength of 2-carboxamide-1,4-di-N-oxide-Quinoxaline derivatives measured by the N-O bond dissociation enthalpies (BDEs) is initially investigated by DFT calculation. Also, in this study, was correlated N-O BDEs to reported experimental inhibition constants.

#### Theory and computational details

Several important molecular properties such as chemical hardness ( $\eta$ ) and electronegativity ( $\chi$ ) have been defined based on the density functional theory [22-25] calculations. Chemical hardness, has been used as a tool to understand the chemical reactivity and some other properties of a molecular system, has been shown that stability of molecules is related to its chemical hardness [26]. The concept of electronegativity has been introduced as the power of an atom in a molecule to attract electrons onto itself [27]. Chemical hardness ( $\eta$ ), and electronegativity ( $\chi$ ) are defined as follows [22-25, 28]:

$$(1) \quad \eta = \frac{1}{2} \left[ \frac{\partial^2 E}{\partial N^2} \right]_{V(r)}$$

$$(2) \quad \chi = - \left[ \frac{\partial E}{\partial N} \right]_{V(r)}$$

Where  $E$  and  $V(r)$  are electronic energy and external potential of an N-electron system, respectively. Using Koopmans' theorem for closed-shell molecules,  $\eta$  and  $\chi$  can be redefined as

$$(3) \quad \eta \approx -\frac{1}{2}(\epsilon_{LUMO} + \epsilon_{HOMO}) \approx \frac{1}{2}(I - A)$$

$$(4) \quad \chi \approx \frac{1}{2}(\epsilon_{HOMO} - \epsilon_{LUMO}) \approx -\frac{1}{2}(I + A)$$

$$I \approx -\epsilon_{HOMO} \quad A \approx \epsilon_{LUMO}$$

Where  $I$  and  $A$  are the ionization potential and electron affinity of the molecules, respectively.  $I$  characterize the susceptibility of a molecule, whereas  $A$  refers to the capability of a ligand to accept precisely one electron from a donor. Electrophilicity ( $\omega$ ) has been proposed as a measure of lowering of energy due to maximal electron flow between the donor and the acceptor [24]. It can be defined as:

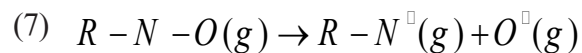
$$(6) \quad \omega = -\frac{\chi^2}{2\eta}$$

This study has also included HOMO–LUMO energy gap as a quantum mechanical descriptor. There are numerous applications of HOMO–LUMO energy gap in establishing a correlation between the chemical structure

and the biological activity. It is well known that the polarity of a molecule is important for various physicochemical properties. The dipole moment ( $\mu$ ) thus is the most obvious and the most widely used quantity to describe the polarity of a molecule.

### Computational details

In the first step of calculations, conformational analysis of 2CdNOQ was performed to determine the most stable conformer. For all the molecules studied, calculations were performed using the Gaussian 03 quantum chemistry package [29]. Initial geometry optimizations were carried out with the molecular mechanics (MM) method, using the MM+ force fields. The lowest energy conformation of the molecules obtained by the MM method were further optimized by the DFT [30] method by employing Becke's three-parameter hybrid functional (B3LYP) [31] and the 6-31+G (d) basis set. In the calculations, the dipole moment (in debye) of the molecules was directly extracted from the Gaussian 03 output file. The HOMO and LUMO values taken as molecular orbital coefficients (in a.u.) from the output of Gaussian 03 calculation were converted into energy (in eV). Rest of the descriptors was obtained using Eqs. (3) – (6). The N–O BDE is the calculated enthalpy change from the hemolytic bond dissociation reaction:



The mean N-O bond dissociation enthalpy of 2CdNOQ is half of the enthalpy of the following reaction:



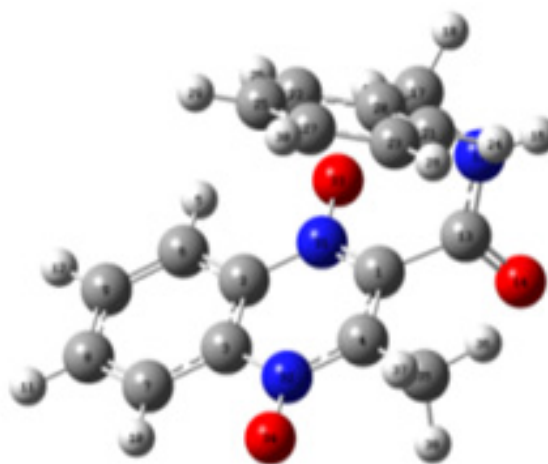
The bond dissociation energy of the N-O bond is computed from the heat formation at 298.15 K of the species involved in the dissociation, i.e.,

$$E_{BDE} = \Delta_f H_{298,R-N}^0 + \Delta_f H_{298,O}^0 - \Delta_f H_{298,R-N-O}^0 \quad (9)$$

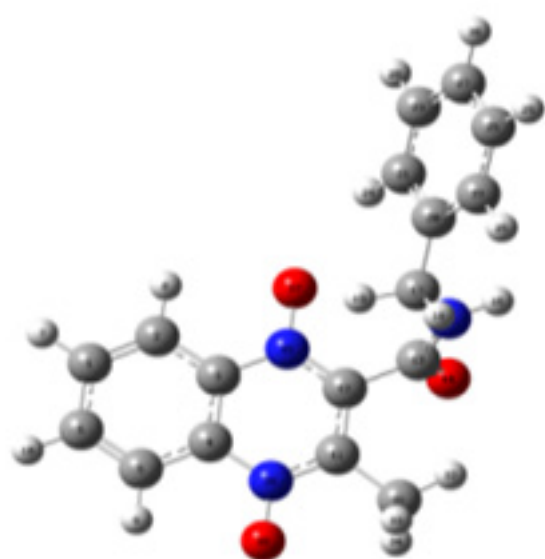
## Results and discussion

### Conformational stability of 2CdNOQ

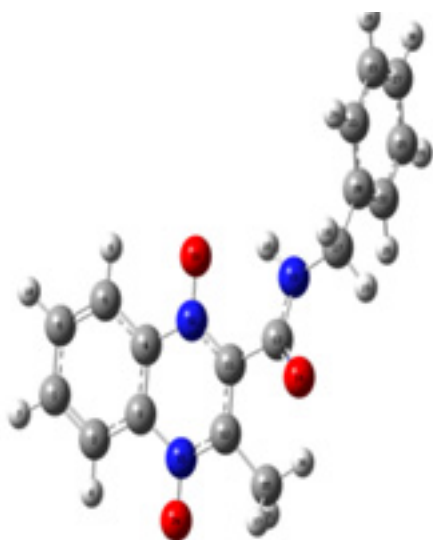
Since the exact crystal structures of these compounds are not available at present, the optimized structures can to assist. We can be said that each of 2CdNOQ derivatives has three staggered conformers (Figure 2).



2CdNOQ-a



2CdNOQ-b



2CdNOQ-c

**Figure 2.** The B3LYP/6-31+G(d) optimized geometric structures for the three conformers of 2CdNOQ molecule ( $R_1=R_2=H$ ).

The B3LYP/6-31+G (d) optimized geometries of these conformers are given in Figure 2 for  $R_1=R_2=H$ . The IC<sub>50</sub> values of the studied compounds were taken from Ref. [21] and

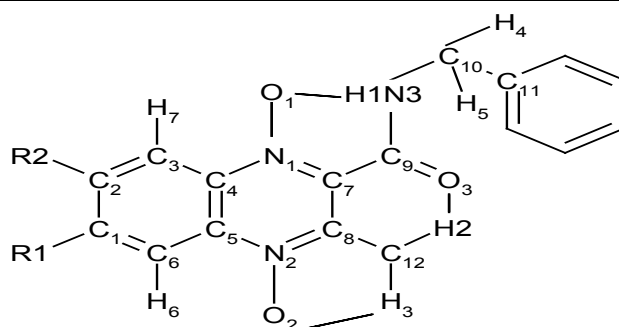
are listed in Table 1. Also, the calculated total electronic energies of each quinoxaline in three forms are presented in this Table. It is evident that 2CdNOQ-c conformer is the most stable form (structure with lowest energy). Among reasons of the stability of this conformer (Figure 3), we can express intramolecular hydrogen bond, according to the data in Table 2. Therefore, in the present work we will focus only in this form of 2CdNOQ molecule to defined molecular structure and assignment of N-O bond dissociation enthalpies (BDEs).

#### *Geometrical structure*

The initial task for the calculation was to determine the optimized geometries of the title compounds. The optimized structural for some geometrical parameters of 2CdNOQ calculated by the DFT-B3LYP level with 6-31+G(d) as the basis sets are listed in Table 3, in accordance with the atom numbering scheme of the c conformer shown in Figure 2. The DFT data show that the C–C bond length is 1.373–1.524 Å. In the case of C–H bonds, C10–H4 of 2CdNOQ is the longest, whereas the C6–H6 and C3–H7 bonds are the shortest, and the rest fall in the range of 1.081–1.097 Å. In addition, N1–O1, N2–O2 and C9–O3 bonds in 2CdNOQ have lengths of 1.296, 1.283, and 1.231 Å, respectively.

**Table 1.** Biological results of the anti-tuberculous screening and calculated energies.

Compounds	R <sub>1</sub>	R <sub>2</sub>	anti-tubercular activity	E <sub>elec</sub> /kJ.mol <sup>-1</sup>
			IC50/μM	
1-a	H	H	4.91	-2748141.86
1-b	H	H	4.91	-2748146.66
1-c	H	H	4.91	-2748161.93
2-a	H	Cl	1.1	-3954804.20
2-b	H	Cl	1.1	-3954808.44
2-c	H	Cl	1.1	-3954823.57
3-a	H	OCH <sub>3</sub>	18.87	-3048831.18
3-b	H	OCH <sub>3</sub>	18.87	-3048835.94
3-c	H	OCH <sub>3</sub>	18.87	-3048851.22
4-a	H	CH <sub>3</sub>	8.35	-2851375.96
4-b	H	CH <sub>3</sub>	8.35	-2851380.56
4-c	H	CH <sub>3</sub>	8.35	-2851396.15
5-a	H	F	2.83	-3008696.51
5-b	H	F	2.83	-3008700.57
5-c	H	F	2.83	-3008715.99
6-a	H	CF <sub>3</sub>	0.81	-3633083.90
6-b	H	CF <sub>3</sub>	0.81	-3633087.83
6-c	H	CF <sub>3</sub>	0.81	-3633102.97

**Figure 3.** General structure of 2CdNOQ with atoms numbering.

**Table 2.** Geometrical data relevant to formation intramolecular hydrogen bond in 2CdNOQ-c.

parameter	1	2	3	4	5	6
Bond length (Å)						
O3...H2	2.255	2.253	2.253	2.261	2.264	2.261
O1...H1	1.912	1.907	1.889	1.901	1.915	1.923
O2...H3	2.439	2.430	2.427	2.427	2.432	2.432
Bond angle (°)						
O3...H2-C12	114.61	114.16	113.93	113.72	113.69	113.81
H2...O3-C9	92.82	93.13	93.18	92.76	92.57	92.68
H1...O1-N1	100.72	100.97	101.06	100.92	100.61	100.76
O1...H1-N3	128.37	128.52	129.13	128.90	128.23	127.82
H3...O2-N2	81.10	81.19	81.26	81.28	81.21	81.13
O2...H3-C12	88.89	89.49	89.73	89.66	89.47	89.42

**Table 3.** Geometrical data of 2CdNOQ.

parameter	1	2	3	4	5	6
Bond length (Å)						
C1-R1	1.086	1.085	1.084	1.087	1.085	1.086
C2-R2	1.086	1.750	1.358	1.509	1.352	1.509
N1-O1	1.296	1.295	1.297	1.297	1.296	1.293
N1-C7	1.361	1.362	1.361	1.362	1.362	1.362
N2-O2	1.283	1.283	1.284	1.284	1.283	1.283
N2-C8	1.361	1.362	1.360	1.362	1.362	1.363
C9-N3	1.353	1.352	1.353	1.353	1.352	1.352
C9-O3	1.231	1.231	1.232	1.231	1.231	1.231
N3-H1	1.019	1.019	1.020	1.020	1.019	1.019
N3-C10	1.465	1.467	1.465	1.464	1.466	1.466

## Bond angle (°)

C4-N1-C7	119.26	119.18	119.31	119.27	119.18	119.09
C5-N2-C8	119.78	119.72	119.71	119.71	119.74	119.66
C7-C9-O3	119.33	119.31	119.49	119.35	119.18	119.11
C8-C12-H2	111.88	111.82	111.79	111.84	111.83	111.88
C8-C12-H3	108.54	108.54	108.56	108.53	108.56	108.51
O3-C9-N3	123.85	123.76	123.66	123.82	123.96	123.96
C9-N3-H1	115.69	115.96	115.63	115.56	115.82	116.05
O1-N1-C7	122.91	123.08	123.13	122.88	123.09	123.02
O2-N2-C8	121.08	121.17	121.15	121.10	121.16	121.21
C9-N3-C10	120.74	120.49	120.47	120.72	120.75	120.72

## Dihedral angle (°)

O1-N1-C7-C9	7.31	7.16	6.99	7.35	7.50	7.48
N1-C7-C9-O3	144.63	145.50	146.03	145.12	144.57	144.62
O2-N2-C8-C12	2.38	2.50	2.57	2.51	2.43	2.49
C8-C7-C9-O3	-32.43	-31.59	-31.21	-31.84	-32.30	-32.24
O3-C9-N3-C10	-5.21	-5.02	-5.27	-5.47	-5.22	-4.91
O3-C9-N3-H1	-160.80	-161.00	-160.68	-160.82	-161.01	-161.16

In 2CdNOQ, the calculated values of the C–C–C angles for the benzene ring are around the typical hexagonal angle of 120, in contrast to the quinoxaline ring, in which the substitution leads to some changes in the bond angles. C5–N2–C8 and C4–N1–C7 in 2CdNOQ show an obvious deviation from 120. The benzene ring and quinoxaline moiety are essentially planar, as evident in the dihedral angles of C5–C4–N1–C7 and C6–C5–N2–C8 are 177.466 and 178.947 for 2CdNOQ.

*Descriptors of molecule and QSAR*

Biological activity is the result of chosen

molecular species interacting with a biological entity. In clinical studies, human organism represents biological entity and in pre-clinical trials, it is the experimental animals (in vivo) or experimental models (in vitro). Biological activity depends on the nature of compound (structure and physicochemical properties), biological entity (species, sex, age, etc.) and mode of treatment (dose, route, etc.) [32]. The biological activities can be defined and determined in organism, organ/tissue and cellular and molecular levels [32]. Approaches to evaluate the compounds with analogous activity are conceptually based on the idea that



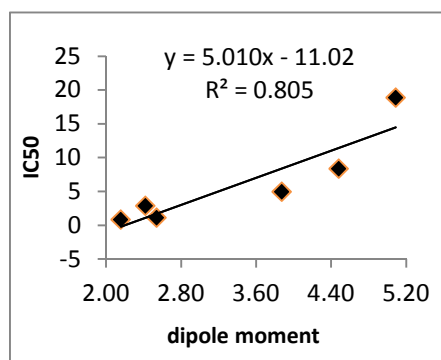
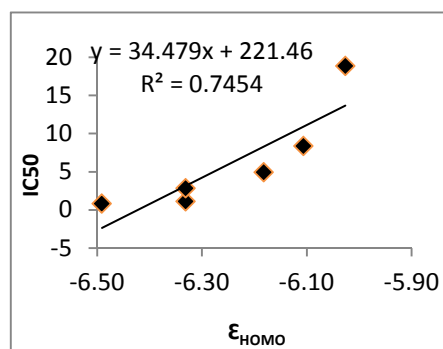
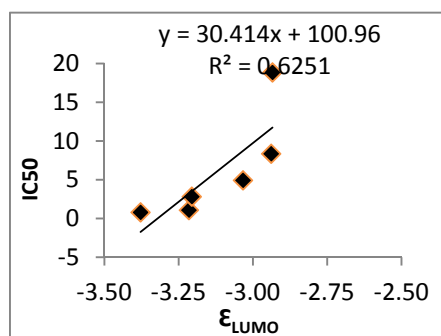
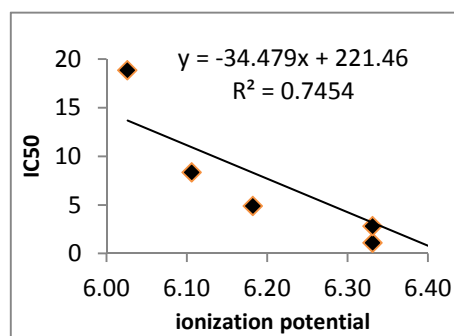
significant similarities in molecular structure and properties are responsible for the same biological activity. However, structure and activity can be obtained in many different ways/sources and it is difficult to generate general molecular representations that capture structure–activity relationships for various sets of molecules. Since there are several descriptors employed to build structure–activity relationship (QSAR), the selection of appropriate descriptors for such generalized QSAR model is a vast task and in general a large number of descriptors are to be used to get a satisfactory correlation. In order to obtain a generalized model for QSAR, the structure–activity relationship has been developed in the present work for 2-carboxamide-1,4-di-N-oxide-Quinoxaline derivatives with the help of conceptually descriptors, such as  $\epsilon_{\text{HOMO}}$ ,  $\epsilon_{\text{LUMO}}$ , dipole moment, energy, electrophilicity, ionization potential, hardness and etc. The negative coefficient of  $\mu$  indicates that the higher the dipole moment, the greater is the activity. The dipole moment is a measure of the molecular polarity, which seems to have an important effect on the activity of 2CdNOQ. According to QSAR model,  $\chi$  has the highest positive coefficients; highlighting the fact that strength of molecular association by charge transfer plays an important role between 2CdNOQ molecules and the receptor TB isozyme. According to Eq. 5.1 equal to  $-\epsilon_{\text{HOMO}}$  and the electron affinity  $A$  is the

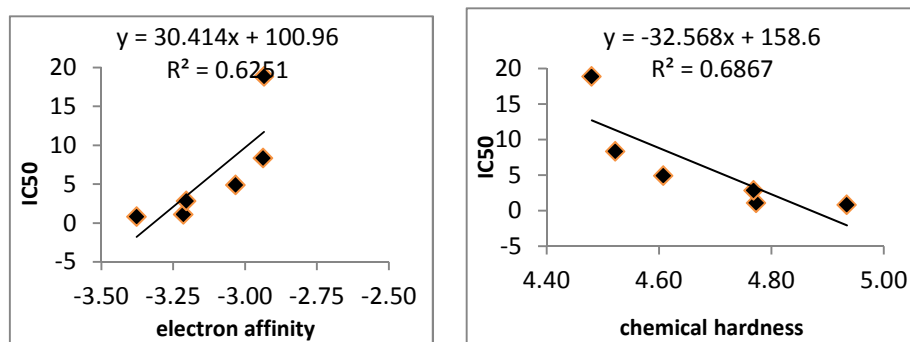
$\epsilon_{\text{LUMO}}$ . This shows that the energies of the frontier molecular orbital (HOMO) affect the inhibition activity.  $\epsilon_{\text{HOMO}}$  is responsible for the formation of charge transfer in a chemical reaction and characterizes the susceptibility of the molecule towards attack by electrophiles. In much, the same role  $\epsilon_{\text{LUMO}}$  also characterizes the susceptibility of the molecule, but towards attack by nucleophiles. It may be said that due to the existence of  $\epsilon_{\text{HOMO}}$  or  $\epsilon_{\text{LUMO}}$  in obtained model, charge transfer between 2CdNOQ molecules and the receptor TB is a dominant factor for modeling the inhibition activity in QSAR. The quantum mechanical descriptors, which were used to build QSAR models, presented in Table 4. Relationship between the calculated descriptors of 2CdNOQ and biological activities, QSAR, has been presented in Figure 3. It is clear from Figure 3 that the descriptors exhibit linear correlation with the biological activities. In this regard electron affinity ( $A$ ) is used as a descriptor to understand the toxicity.

**Table 4.** DFT-based calculated molecular descriptors and predicted inhibition activities of quinoxaline compounds.

compound	$\mu$	$\epsilon_{HOMO}$	$\epsilon_{LUMO}$	$\epsilon_L - \epsilon_H$	$I$	$A$	$\chi$	$\eta$	$\omega$	IC50/ $\mu$ M
1	3.87	-6.18	-3.03	3.15	6.18	-3.03	-1.57	4.61	-0.27	4.91
2	2.54	-6.33	-3.22	3.12	6.33	-3.22	-1.56	4.77	-0.25	1.1
3	5.09	-6.03	-2.93	3.09	6.03	-2.93	-1.55	4.48	-0.27	18.87
4	4.48	-6.11	-2.94	3.17	6.11	-2.94	-1.58	4.52	-0.28	8.35
5	2.42	-6.33	-3.21	3.13	6.33	-3.21	-1.56	4.77	-0.26	2.83
6	2.16	-6.49	-3.38	3.11	6.49	-3.38	-1.56	4.93	-0.25	0.81

IC50, observed inhibition constant ( $\mu$ M);  $\mu$ , dipole moment (debye);  $\epsilon_{LUMO}$ , energy of LUMO (eV);  $\epsilon_{HOMO}$ , energy of HOMO (eV);  $\epsilon_L - \epsilon_H$ , energy difference between HOMO and LUMO (eV);  $I$ , ionization potential (eV);  $A$ , electron affinity (eV);  $\chi$ , electronegativity (eV);  $\eta$ , chemical hardness (eV);  $\omega$ , electrophilicity (eV)

Plot of observed IC50 versus calculated  $\mu$ Plot of observed IC50 versus calculated  $\epsilon_{HOMO}$ Plot of observed IC50 versus calculated  $\epsilon_{LUMO}$ Plot of observed IC50 versus calculated  $I$



Plot of observed IC50 versus calculated A

Plot of observed IC50 versus calculated  $\eta$ 

**Figure 4.** The linear regression between observed inhibition constant (IC50) and DFT-based calculated molecular descriptors of title compounds.

### *N-O BDE calculation*

The N–O BDE is defined as the enthalpy change of the dissociation reaction in the gas phase at 298.15 K and 1 atm. 2CdNOQ has two different N–O bonds, one closer to the methyl group, and the other closer to the carboxamide group. Due to the different chemical neighborhoods, these bonds are expected to have different strengths and dissociation energies. Consequently, the N–O BDE may be described in terms of the first, second, total, and mean N–O BDE values.

In this study, the first, second, total, and mean N–O BDE of 2CdNOQ are calculated in B3LYP/6-31+G(d) level of theory. The first N–O BDE is the energy required to break the weakest bonds in the di-N-oxide compound to yield the corresponding N-oxide. The second N–O BDE is the energy required to break the bond in the N-oxide compound to yield the parent quinoxaline. The total N–O BDE and the mean N–O BDE are the sum and mean

of the former two dissociation enthalpies, respectively.

The calculated values for the BDE of 2CdNOQ are schematically depicted in Figure 5. The dissociation of the N(1)-O(1) bond, which is closer to the branched chain, occurred easily than the N(2)-O(2) bond and yielded a first N–O BDE value of 545.05 kJ mol<sup>-1</sup> (Figure 5). Second N–O BDE, the energy required to remove the O(2) atom was 551.13 kJ mol<sup>-1</sup>, almost 6 kJ mol<sup>-1</sup> higher than the first N–O BDE.

The corresponding value of the total and mean N–O BDE was 1105.04 and 552.52 kJ mol<sup>-1</sup>, respectively. N–O BDEs for this molecule presented in Table 5. Also, exist linear regression between calculated N–O BDEs to reported experimental inhibition constants, according to Figure 5.

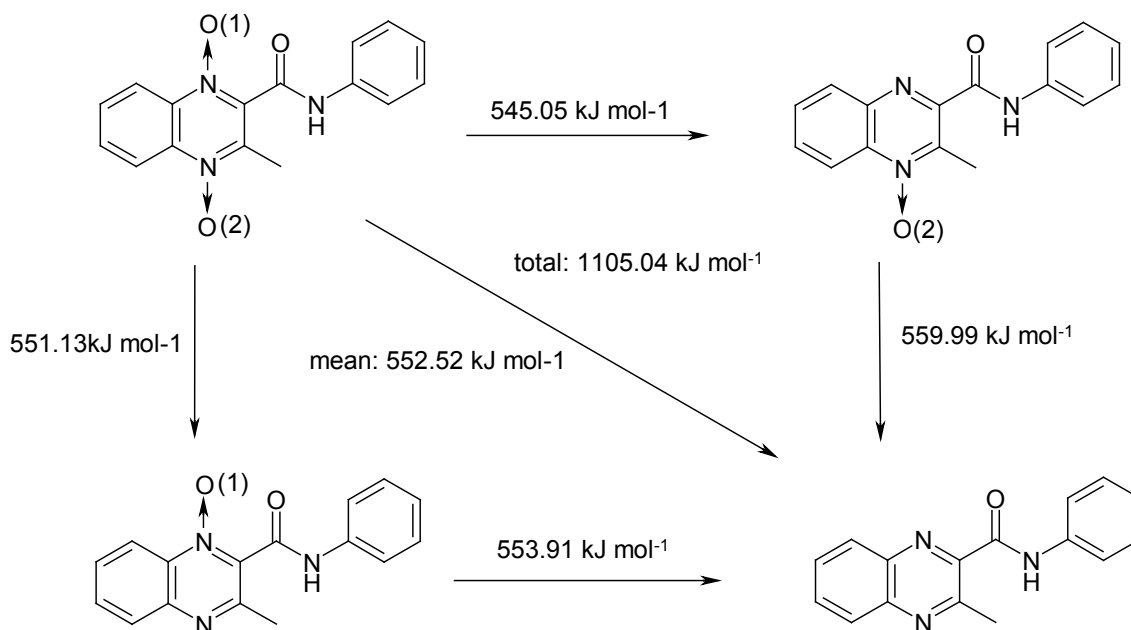
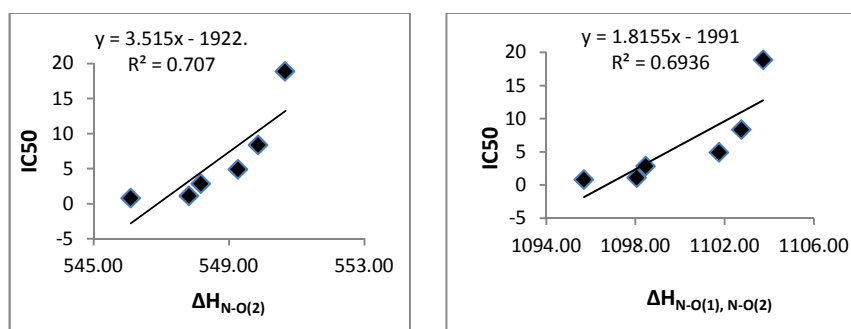


**Figure 5.** First, second, total and mean N–O BDEs for 2CdNOQs were computed at the B3LYP/6-31+G(d) level of theory.

**Table 5.** DFT-based calculated N-O BDEs of title compounds.

compound	$\Delta H_{N-O(1)}$	$\Delta H_{N-O(2)}$	$\Delta H_{N-O(1), N-O(2)}$	IC <sub>50</sub> /μM
1	546.53	551.76	1106.71	4.91
2	544.16	550.30	1103.03	1.1
3	544.98	553.15	1108.69	18.87
4	547.33	552.35	1107.71	8.35
5	544.23	550.66	1103.42	2.83
6	543.10	548.58	1100.65	0.81

IC<sub>50</sub>, observed inhibition constant (μM);  $\Delta H_{N-O(1)}$ , N1– O1 BDE (kJ mol<sup>-1</sup>);  $\Delta H_{N-O(2)}$ , N2– O2 BDE (kJ mol<sup>-1</sup>);  $\Delta H_{N-O(1), N-O(2)}$ , N1– O1 and N2– O2 BDE (kJ mol<sup>-1</sup>).



Plot of observed IC<sub>50</sub> versus calculated  $\Delta H_{N-O(2)}$

Plot of observed IC<sub>50</sub> versus calculated  $\Delta H_{N-O(1), N-O(2)}$

**Figure 6.** The linear regression between observed inhibition constant (IC<sub>50</sub>) and DFT-based calculated N-O BDEs of title compounds.

## Conclusion

In this study, the most stable conformer of 2-carboxamide-1,4-di-N-oxide-Quinoxaline molecule were obtained and used to calculate of quantum mechanical descriptor of 2CdNOQ derivatives at the DFT/B3LYP/6-31+G (d) level of the theory. The DFT-based descriptors were applied to drive the QSAR models by which the calculated quantum mechanical parameters were correlated to activity of compounds taken from the literature [21]. The inhibition activity is highly influenced by the polarity of the molecules. The authors believe that the models introduced in this study can be used to estimate the inhibition activity of novel 2CdNOQ compounds of this series, prior to synthesis by calculating the descriptors involved in these equations. Moreover, the first, second, total, and mean N-O bond dissociation enthalpies (BDEs) were obtained theoretically. The predicted values based on 6-31+G(d) were 545.05, 551.13, 1105.04, and 552.51 kJ mol<sup>-1</sup>, respectively. Also, exist linear regression between calculated N-O BDEs to reported experimental inhibition constants.

## Acknowledgments

We would like to thank Islamic Azad University, Karaj Branch and South Tehran Branch for their supports to this work.

## References

- [1] J. C. Grossman, L. Mitas, K. Raghavachari, *Phys. Rev. Lett.*, 75, 3870 (1995).
- [2] WHO, *Weekly Epidemiological Record*, 78, 121 (2003).
- [3] J.C. Palomino, S.C. Leao, V. Ritacco, *Tuberculosis: From Basic Science to Patient Care*, <http://www.tuberculosis-textbook.com> (2007).
- [4] R. C. Goldman, B. E. Laughon, R. C. Reynolds, J. A. Secrist, J. A. Maddry, M. A. Guie, A. C. Poffenberger, C. A. Kwong, S. Ananthan, *Disord. Drug Targets*, 7, 92 (2007).
- [5] E. Vicente, R. Villar, B. Solano, A. Burguete, S. Ancizu, S. Pérez-Silanes, I. Aldana, *A. R. Acad. Nac. Farm.*, 73, 927 (2007).
- [6] G. Aguirre, V. Cerecetto, R. Di Maio, M. Gonzalez, M. E. M. Alfaro, A. Jaso, B. Zarranz, M. A. Ortega, I. Aldana, A. Monge-Vega, *Bioorg. Med. Chem. Lett.* 14, 3835 (2004).
- [7] C. Urquiola, M. Vieites, G. Aguirre, A. Marin, B. Solano, G. Arrambide, P. Noblia, M. L. Lavaggi, M. H. Torre, M. Gonzalez, A. Monge, D. Gambino, H. Cerecetto, *Bioorg. Med. Chem.*, 14, 5503 (2006).
- [8] A. Carta, M. Loriga, G. Paglietti, A. Mattana, Fiori P.L., Mollicotti P., Sechi L., Zanetti S., *Eur. J. Med. Chem.*, 39, 195 (2004).
- [9] B. Ganley, G. Chowdhury, J. Bhansali, J. S. Daniels, K. S. Gates, *Bioorg. Med. Chem.*, 9, 2395 (2001).
- [10] S. Ancizu, E. Moreno, B. Solano, R. Villar, A. Burguete, E. Torres, S. Pérez-Silanes, I. Aldana, A. Monge, *Bioorg. Med. Chem.*, 18,

2713 (2010).

- [11] C.Hansch,A.Leo, Exploring QSAR. *Fundamentals and Applications in Chemistry and Biology*, American Chemical Society, Washington, DC, 89 (1995).
- [12] R.P.Verma,C.Hansch, *Chem. Biochem.*, 5, 1188 (2004).
- [13]C. Hansch,A. Leo,R. W.Taft, *Chem. Rev.*, 91, 165 (1991).
- [14]H. Gao,J. A.Katzenellenbogen,R.Garg, C. Hansch, *Chem. Rev.*, 99, 723 (1999).
- [15]R. Franke, Theoretical Drug Design Methods, Elsevier:Amsterdam, New York, 115 (1984).
- [16]S. P. Gupta,P. Singh,M. C.Bindal, *Chem. Rev.*, 83, 633 (1983).
- [17]S. P. Gupta, *Chem. Rev.*, 91, 1109 (1991).
- [18]M. Karelson,V. S.Lobanov,A. R.Katritzky, *Chem. Rev.*, 96, 1027 (1996).
- [19]M. T. D.Cronin, *Current Opinion in Drug Discovery and Development*, 3, 292 (2000).
- [20]A.R. Katritzky,V.S. Lobanov,M. Karelson, *Chem. Soc. Rev.*, 24, 279 (1995).
- [21]E.Torres,E. Moreno,S. Ancizu,C. Barea,S. Galiano,I. Aldana,A.Monge,S.Perez-Silanes, *Bioorg. Med. Chem. Lett.*, 21, 3699 (2011).
- [22]R.G. Parr,R.A. Donnelly,M. Levy,W.E. Palke, *J. Chem. Phys.*, 68, 3801 (1978).
- [23]R.G. Parr,R.G. Pearson, *J. Am. Chem. Soc.*, 105, 7512 (1983).
- [24] R.G. Parr, L.V. Szentpaly, S. Liu, *J. Am. Chem. Soc.*,121, 1922 (1999).
- [25]R.G. Parr,P.K. Chattaraj, *J. Am. Chem. Soc.*, 113, 1854 (1991).
- [26]Z. Zhou,R.G. Parr, *J. Am. Chem. Soc.*, 112, 5720 (1990).
- [27]I. Pauling, The Nature of the Chemical Bond and the Structure of Molecules and Crystals: *An Introduction to Modern Structural Chemistry*, 3rd ed., Cornell University Press, Ithaca, NY (1960).
- [28]R.G. Pearson, Z.B. (Ed.) Maksic, Theoretical Models of Chemical Bonding Part II, *Springer, Berlin*, 45 (1990).
- [29]M. J. Frisch, G. W. Trucks, H. B. Schlegel, G. E. Scuseria, M. A. Robb, J. R. Cheeseman, J. A. Montgomery, Jr., T. Vreven, K. N. Kudin, J. C. Burant, J. M. Millam, S. S. Iyengar, J. Tomasi, V. Barone, B. Mennucci, M. Cossi, G. Scalmani, N. Rega, G. A. Petersson, H. Nakatsuji, M. Hada, M. Ehara, K. Toyota, R. Fukuda, J. Hasegawa, M. Ishida, T. Nakajima, Y. Honda, O. Kitao, H. Nakai, M. Klene, X. Li, J. E. Knox, H. P. Hratchian, J. B. Cross, V. Bakken, C. Adamo, J. Jaramillo, R. Gomperts, R. E. Stratmann, O. Yazyev, A. J. Austin, R. Cammi, C. Pomelli, J. W. Ochterski, P. Y. Ayala, K. Morokuma, G. A. Voth, P. Salvador, J. J. Dannenberg, V. G. Zakrzewski, S. Dapprich, A. D. Daniels, M. C. Strain, O. Farkas, D. K. Malick, A. D. Rabuck, K. Raghavachari, J. B. Foresman, J. V. Ortiz, Q. Cui, A. G. Baboul, S. Clifford, J. Cioslowski, B. B. Stefanov, G. Liu, A. Liashenko, P. Piskorz, I. Komaromi, R. L. Martin, D. J. Fox, T. Keith, M. A. Al-Laham, C. Y. Peng, A. Nanayakkara, M. Challacombe,

P. M. W. Gill, B. Johnson, W. Chen, M. W. Wong, C. Gonzalez, and J. A. Pople, *Gaussian, Inc.*, Wallingford CT (2003).

[30] G.Parr, W. Yang, *Density-Functional Theory of atoms and molecules*. Oxford Univ, Press: Oxford (1989).

[31] A. D. Becke, *J. Chem. Phys.*, 98, 5648 (1993).

[32] D. A. Filimonov, V. V.Poroikov, PASS: Computerized Prediction of Biological Activity Spectra for Chemical Substances. *In Bioactive Compound Design: Possibilities for Industrial Use*, BIOS Scientific: Oxford, 47 (1996).